ELSEVIER
Biophysical Chemistry 123 (2006) 102–112
Biophysical Chemistry
http://www.elsevier.com/locate/biophyschem

Electrochemical and ligand binding studies of a de novo heme protein

Aditi Das [a,1], Scott A. Trammell [b], Michael H. Hecht [a,*]

[a] Department of Chemistry, Princeton University, Princeton, NJ 08544-1009, United States
[b] Center for Bio/Molecular Science and Engineering, Naval Research Laboratory, Washington, DC 20375, United States

Received 28 March 2006; accepted 20 April 2006
Available online 29 April 2006

Abstract

Heme proteins can perform a variety of electrochemical functions. While natural heme proteins carry out particular functions selected by biological evolution, artificial heme proteins, in principle, can be tailored to suit specified technological applications. Here we describe initial characterization of the electrochemical properties of a de novo heme protein, S824C. Protein S824C is a four-helix bundle derived from a library of sequences that was designed by binary patterning of polar and nonpolar amino acids. Protein S824C was immobilized on a gold electrode and the formal potential of heme–protein complex was studied as a function of pH and ionic strength. The binding of exogenous N-donor ligands to heme/S824C was monitored by measuring shifts in the potential that occurred upon addition of various concentrations of imidazole or pyridine derivatives. The response of heme/S824C to these ligands was then compared to the response of isolated heme (without protein) to the same ligands. The observed shifts in potential depended on both the concentration and the structure of the added ligand. Small changes in structure of the ligand (e.g. pyridine versus 2-amino pyridine) produced significant shifts in the potential of the heme–protein. The observed shifts correlate to the differential binding of the N-donor molecules to the oxidized and reduced states of the heme. Further, it was observed that the electrochemical response of the buried heme in heme/S824C differed significantly from that of isolated heme. These studies demonstrate that the structure of the de novo protein modulates the binding of N-donor ligands to heme.

Keywords: Protein design; Binary patterning; Cyclic voltammetry; Redox protein; Heme protein

1. Introduction

Proteins have the ability (i) to bind target compounds with high affinity and exquisite selectivity, and (ii) to signal such binding events by a variety of mechanisms. These properties render proteins ideally suited for use in a variety of sensing applications. Redox proteins are particularly attractive as sensors because changes induced by ligand binding can be detected optically and/or electrochemically, thereby obviating the need for additional detection reagents [1–4].

Naturally occurring proteins, however, have several drawbacks that can limit their usefulness in technological applications. Natural proteins were selected by evolution to perform specific functions in particular biological environments. Because these functions–and the environments in which they evolved–may differ substantially from those required by technological applications, the 'evolutionary baggage' associated with natural proteins may render them unsuitable for incorporation into sensors or other devices. For these reasons, we have begun to explore the electrochemical properties of artificial redox proteins.

Our initial studies, reported herein, focus on the de novo protein S824C. This protein is a variant of sequence S824, which was chosen from a library of 102-residue proteins designed to fold into four-helix bundles [5,6]. This library was designed using the 'binary code' strategy, in which each position in an amino acid sequence is designed to be either polar or nonpolar, but the exact identity of each polar and nonpolar residue is not specified, and is varied combinatorially [7–9]. Initial characterization of several proteins chosen arbitrarily from this library showed that the majority of them form well-folded and/or native-like structures [5,6].

* Corresponding author. Tel.: +1 609 258 2901; fax: +1 609 258 6746.
E-mail address: hecht@princeton.edu (M.H. Hecht).
[1] Current Address: Beckman Institute of Advanced Science and Technology, University of Illinois-Urbana Champaign, United States.

0301-4622/$ - see front matter © 2006 Elsevier B.V. All rights reserved.
doi:10.1016/j.bpc.2006.04.011

The de novo proteins devised by the binary code strategy were not explicitly designed to bind heme. Nonetheless, protein S824 and several other proteins from the libraries do in fact bind heme [10]. We have shown previously that these de novo heme proteins (i) readily cycle between oxidized and reduced states; (ii) bind reversibly to small ligands (e.g. CO); and (iii) in some cases catalyze redox (e.g. peroxidase) chemistry [11–13].

The 3-dimensional structure of protein S824 was solved at high resolution and shown to be a well-ordered four-helix bundle [6]. Because this structure was determined in the absence of heme, the structural details of heme binding are not known. However, given the well-packed core of apo-S824, binding of the heme macrocycle must produce some structural rearrangements. In the resulting heme–protein structure, the heme is unlikely to be fully sequestered in the hydrophobic core. The resulting access to water presumably accounts for the relatively low reduction potential of S824 [13].

The reduction potential of heme/S824 was shown previously to be −0.374 V (vs. Ag/AgCl). (The value was reported as −0.174 V versus NHE [13].) This suggests that histidine (rather than methionine) binds the heme iron [13]. (Cysteine can be excluded because it does not occur in the sequence of S824.) The sequence of S824 contains 12 histidines, and these polar side chains are exposed to solvent in the NMR structure of the apo-protein (Fig. 1). Upon heme binding, structural reorganization presumably moves histidines side chains into positions consistent with binding to the partially buried macrocycle.

For the current studies, protein S824 was attached to a gold electrode via an engineered Gly–Gly–Cys linker at the C-terminal end. (The terminally modified protein is called S824C.) Heme was bound to the protein and the electrochemical response of this immobilized heme–protein was studied as a function of pH and ionic strength. Further, the electrochemical response of heme/S824C to added N-donor ligands was measured for a series of imidazole derivatives and pyridine derivatives. To assess the role of the protein structure on the properties of the bound heme, we compared our electrochemical and ligand binding results for heme/S824C with those obtained for isolated heme (without protein) immobilized on a gold electrode.

2. Results

2.1. Immobilization and characterization of de novo heme protein S824C

2.1.1. Attachment of the heme protein to a gold electrode

To facilitate attachment of the protein to a gold electrode, we modified the original sequence S824 by elongating the gene to encode a Gly–Gly–Cys tripeptide at the C-terminus of the protein. The new protein is called S824C. Our method for attaching S824C to the gold electrode is shown schematically in Fig. 2. Initially, the electrode was coated with a cystamine monolayer. The coated electrode was then reacted with the bifunctional reagent *N*-succinimidyl-3-maleimidopropionate to yield a maleimide functionalized electrode [14]. The resulting electrode was then reacted with S824C to yield the immobilized four-helix bundle. Finally, the immobilized protein was treated with Fe (III) protoporphyrin IX to generate the immobilized heme protein, as shown in Fig. 2.

2.1.2. Cyclic voltammetry of the immobilized heme protein

As shown in Fig. 3, cyclic voltammetry of heme/S824C immobilized on a gold electrode revealed a single redox wave with a formal potential (vs. Ag/AgCl/KCl) of $E°=-0.350$ V. The formal potential was calculated as the average of the cathodic and anodic peak potentials in the cyclic voltammogram (CV).

The observed formal potential for heme/S824C immobilized on the gold electrode is in close agreement with the

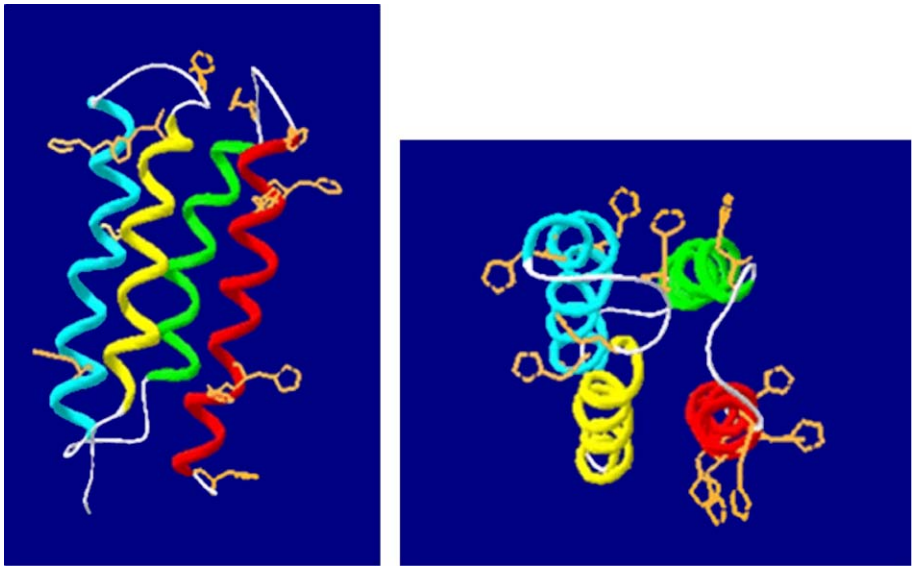

Fig. 1. (a) Ribbon diagram of the four helix bundle protein S824 showing the placement of histidine residues. (b) Head-on view of the structure showing the 12 histidine residues in orange. Note that most of the histidine residues in the apo-protein are exposed to the solvent, as specified by the binary code strategy. The NMR structure was determined in the apo form by Wei et al. [6].

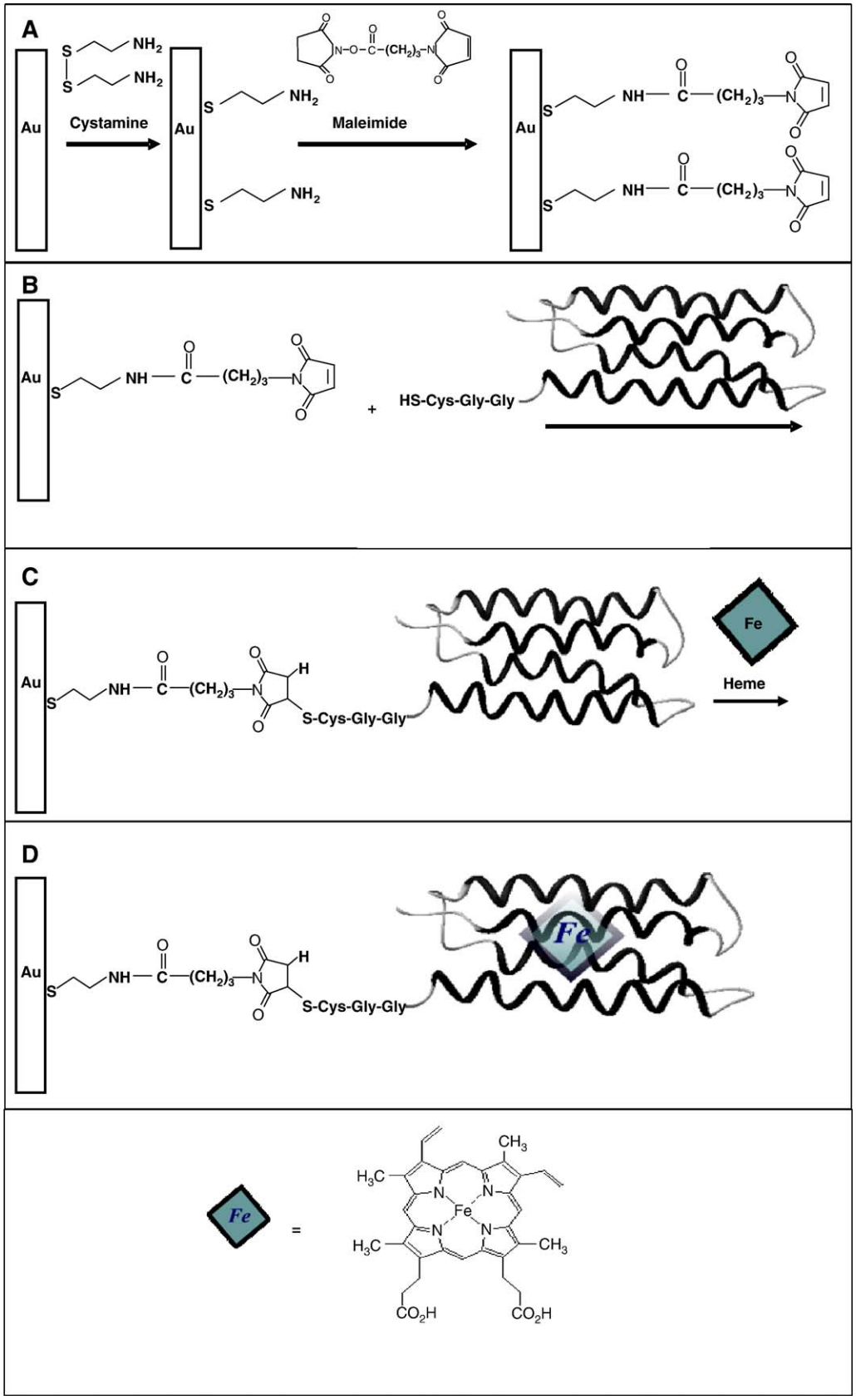

Fig. 2. Stepwise assembly of the S824C/heme protein onto a gold electrode.

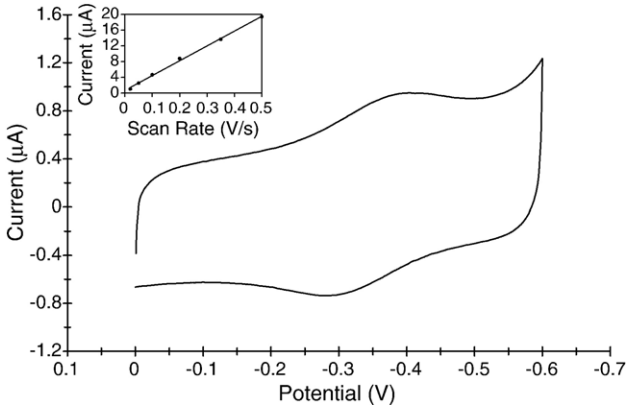

Fig. 3. Cyclic voltammogram of the heme/S824C immobilized on a gold electrode. The scan rate is 0.02 V/s. The redox potential is −0.350 V (versus Ag/AgCl/KCl). The inset shows a plot of the peak cathodic current against the scan rates varying from 0.02 to 0.5 V/s. The plot is linear as expected for a surface immobilized species.

potential reported previously for heme/S824 determined in solution by potentiometric titration [13]. This indicates that attachment to the electrode yields a heme–protein complex similar to that obtained in solution. The plot of current vs. scan rate shown in the inset of Fig. 3 is linear and increases with increasing scan rate, as is typical for surface immobilized species [15,16].

2.1.3. Dependence of the midpoint potential on pH and ionic strength

The formal potential for the electrochemical response of heme/S824C is dependent on pH, as shown in Fig. 4. The experimental data were fitted to a function involving the titration of two groups, with different pK_a values in either oxidation state [17]. The pK_a's obtained from the fit are 6.08 and 6.77 (oxidized) and 6.64 and 8.40 (reduced). The pH profile of the de novo heme–protein is similar to natural cytochromes, which typically have pK_a values in the range of 6–7 [18].

The redox peaks diminish below pH 5.5 and are unobservable at pH 4.5. At low pH, protonation of the ligating amino acid residues would diminish heme binding. Moreover, the surface itself can become protonated, which would disrupt electrostatic interactions between the protein and the electrode. Similarly, above pH 8.0 both redox peaks diminish. This could be due to deprotonation of ligating amino acid residues. The identities of the side chains responsible for the change of E_m with pH are not known since our present knowledge of the structure of S824 is limited to the apo form.

The formal potential of heme/S824C was also studied as a function of ionic strength. The ionic strength was varied from I=128 mM to I=636 mM by adjusting the concentration of sodium phosphate buffer at pH 7.4. Over this range, the peak current increased almost proportional to the ionic strength. However, the midpoint potential of the heme–protein did not change significantly. This behavior can be contrasted with most small heme proteins, for which the potentials are typically sensitive to the ionic strength of the surrounding solution [19]. The observed insensitivity of the potential of heme/S-824C to ionic strength suggests the heme in this protein is relatively shielded from solvent.

2.2. Immobilization and characterization of isolated heme

To assess the role of the de novo protein scaffold on the electrochemical behavior of the heme protein, we sought to establish default values using immobilized heme in the absence of protein. This immobilized heme is hereafter referred to as "isolated heme." Isolated heme was attached to a gold surface as described below, and its electrochemical response was measured and compared with that of heme/S824C.

2.2.1. Attachment of isolated heme to gold electrode

The method for attaching heme to the gold electrode is shown schematically in Fig. 5 [20]. Initially, the gold electrode was coated with alkyl-thiols. A mixture of alkyl-thiols was used such that a small percentage of them bore an activated functional group (3,3′-dithiopropionic acid di-(*N*-succinimidyl ester) for subsequent attachment of heme (see figure). To ensure that hemes in the final product were independently reconstituted with protein, only a small fraction of the thiols contained this activated group. The coated gold electrode was then reacted with 1,12 diaminododecane, which reacts with the thiols bearing activated functional groups. Finally, the amine terminated groups were covalently coupled to the carboxyl groups on Heme (Fe (III) protoporphyrin IX), using EDC (1-ethyl-3-(3-dimethylaminopropyl) carbodiimide) coupling agent. The resulting immobilized heme system has significant advantages over free heme in solution, which tends to aggregate and precipitate.

2.2.2. Cyclic voltammetry of immobilized heme

As shown in Fig. 6, the cyclic voltammogram of the heme-modified electrode shows symmetric oxidation and reduction peaks. The formal potential (vs. Ag/AgCl/KCl) is approximately −0.295 V. The plot of peak current vs. scan rate is linear (Fig. 6, inset), and increases with increasing scan rate, as is typical for

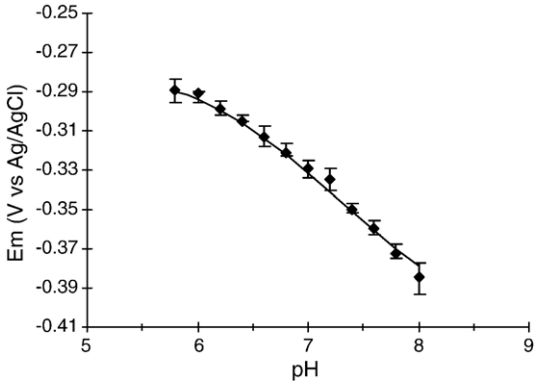

Fig. 4. Formal potential of heme/S824 as a function of pH. Potentials were recorded at 0.02 V/s in a mixed buffer system. Solutions were buffered from pH 4.2 to pH 5.6 with sodium acetate/acetic acid buffer; from pH 5.8 to pH 6.8 with sodium phosphate buffer; and from pH 7 to pH 8.2 with Tris/HCl buffer. All buffers were at an ionic strength equivalent to 50 mM sodium phosphate buffer at pH 7.4.

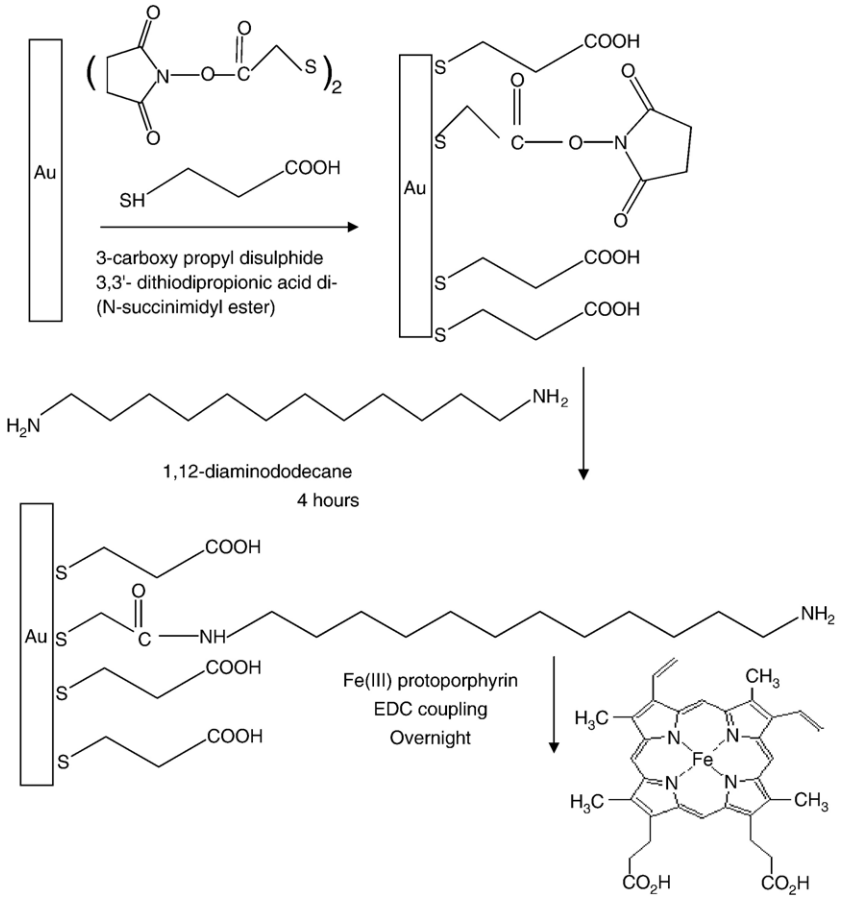

Fig. 5. Schematic representation of immobilization of heme onto a gold electrode.

surface immobilized species [15,16]. The anodic to cathodic peak separation is ~0.111 V compared to 0.080 V in the heme protein CV shown in Fig. 3.

2.3. Electrochemical response to the binding of N-donor ligands

Earlier studies of heme/S824 showed that it bound carbon monoxide [12], thereby demonstrating that the heme iron had a displaceable axial ligand. The kinetics of CO association indicated that the heme in S824 was partially buried [12], consistent with the insensitivity of the formal potential to ionic strength (see above). The ability of the heme in S824 to bind CO in a semi-buried environment suggests that binding of exogenous compounds might shift the potential of this heme protein. To probe this possibility, we characterized the electrochemical response of heme/S824C to the binding of various imidazole and pyridine derivatives. These results are then compared to the binding of the same compounds to isolated heme.

2.3.1. Binding of imidazoles

Fig. 7a shows that the peaks in the CV of heme/S824C are shifted to more negative potential by the presence of imidazole. Similar shifts are seen in Fig. 7b for imidazole binding to isolated heme. To assess how these shifts in the potential are affected by modifications in the structure of the ligand, binding was also evaluated for 1-methyl imidazole, 2-methyl imidazole, and 4-methyl imidazole. As shown in Fig. 8, different imidazole derivatives shifted the potential to different extents—both for heme/S824C and for isolated heme. Moreover, the binding properties of heme/S824C are somewhat different from those of isolated heme. These results demonstrate several important features.

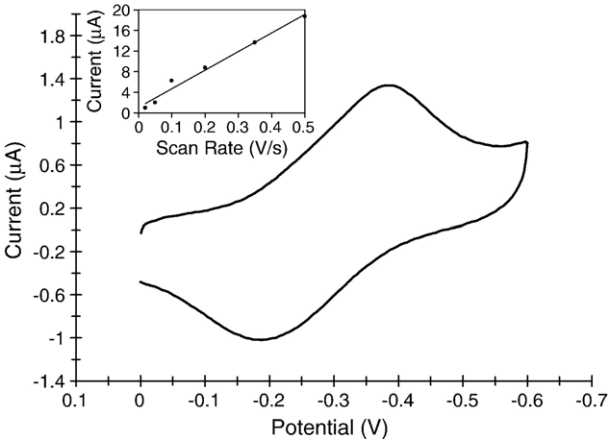

Fig. 6. Cyclic voltammogram of heme-modified electrode in 50 mM phosphate buffer at pH 7.4 at 0.02 V/s scan rates. The inset shows the plot of current vs. scan rate.

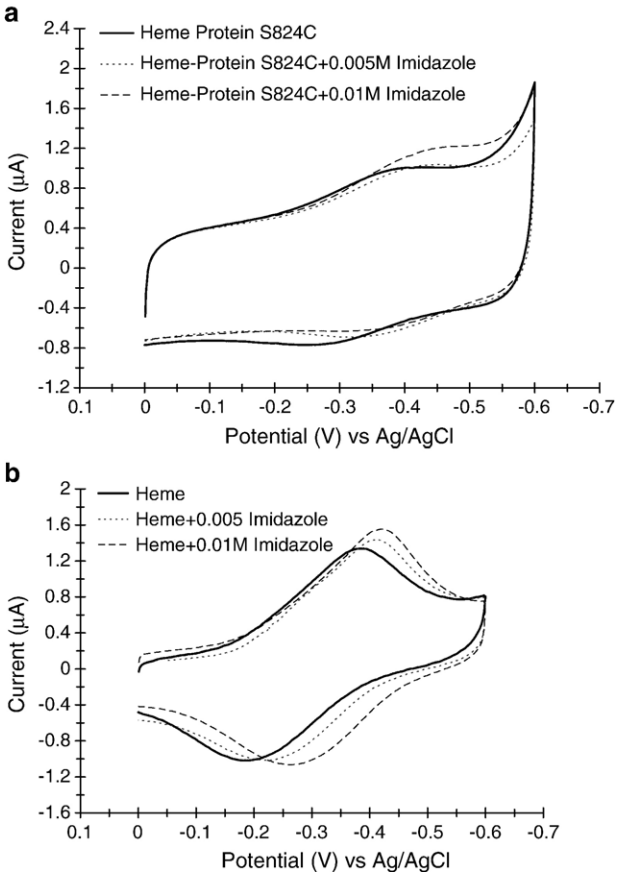

Fig. 7. (a) Cyclic voltammetry of immobilized heme/S824C in the absence (solid) and presence of 0.005 M (dotted) and 0.01 M imidazole (dashed) (scan rate 0.02 V/s). (b) Cyclic voltammetry of immobilized heme in the absence (solid) and presence of 0.005 M (dotted) and 0.01 M imidazole (dashed).

First, both isolated heme and heme/S824C can distinguish between closely related imidazole compounds. The changes in potential of heme/S824C and of isolated heme upon binding to 4 different imidazole derivatives are listed in Table 1. These results demonstrate that both the heme/S-824C protein and the isolated heme system respond differently to imidazole compounds that differ from one another by the presence and location of a single methyl group.

Second, heme/S824C binds both imidazole and 1-methyl imidazole with greater affinity than does isolated heme. This can be seen from the size of the potential shifts. As shown in Fig. 8 and Table 1, imidazole at a concentration of 0.01 M shifts the potential of heme/S824C by −0.096 V, but shifts the potential of isolated heme by only −0.053 V. Likewise, for 1-methyl imidazole (at 0.01 M), ΔE_m is −0.045 for heme/S824C and only −0.020 for isolated heme.

Third, heme/S824C binds 2-methyl imidazole with lower affinity than does isolated heme. This can be seen from the potential shifts in Fig. 8 and Table 1. ΔE_m for 2-methyl imidazole binding to heme/S824C is −0.032 V, while it is −0.090 for binding to the isolated heme. For 4-methyl imidazole, heme/S824C and isolated heme show little difference in binding.

2.3.2. Binding of pyridines

As shown in Figs. 9 and 10, binding of pyridine and three pyridine derivatives (2-aminopyridine, 3-aminopyridine, and 4-cyanopyridine) shifts the reduction potential of heme/S824C and of isolated heme. In contrast to what was observed for the imidazole derivatives, the pyridine derivatives shift the potential in the positive direction.

As was the case for the imidazole derivatives, both heme/S824C and isolated heme readily distinguish the various pyridine derivatives from one another (Fig. 10). Changes in the potential of heme/S824C and of isolated heme in response to the four different pyridine derivatives at 0.01 M concentration are listed in Table 1.

In contrast to what was observed for the imidazole derivatives, heme/S824C binds all the pyridine derivatives less well than does the isolated heme. This is demonstrated by the finding that binding pyridine (and its derivatives) produces smaller shifts in potential for the heme protein than for the isolated heme. These results suggest the protein scaffold may partially block accessibility to the heme. For one derivative, 2-aminopyridine, the protein scaffold seems to prevent binding almost entirely. Thus, when 2-aminopyridine is added at a concentration of 0.01 M, the midpoint potential of isolated heme is shifted by 0.057 V, whereas the midpoint potential of the heme/S-824C protein is nearly unchanged (Table 1).

2.3.3. Effect of ligand binding on the cyclic voltammogram of heme/S824C

As shown in Figs. 7(a) and 9(a), binding of imidazoles and pyridines causes the voltammogram peaks for heme/S824C not only to shift, but also to broaden. The effects on the cathodic and anodic peaks depend on the class of ligand. Imidazole derivatives leave the cathodic peak sharp and shift it to more negative values, while the anodic peak both shifts and broadens. In contrast, addition of pyridine derivatives causes the opposite behavior—the anodic peak remains sharp and shifts to more positive values, while the cathodic peak both shifts and broadens.

The shifts in potential are due to differential binding of ligand by the oxidized and reduced states of heme protein (see Discussion). The observed broadening may indicate that at high concentration of ligand, a second equivalent binds to the heme. The plots in Figs. 8 and 10 for heme–protein S824C indicate that although $m=1$ for low concentrations of ligand, m appears to be ~2 at higher concentration of ligand (m is the number of exogenous ligand molecules bound to the heme). The occurrence of multiple heme-ligated species would cause heterogeneity in the system and lead to the broadening of the peaks.

Protein S824 is known to form a well-packed structure in the apo-state [6]. However, since S824 was not explicitly designed to bind heme, it would not be surprising if the binding site is somewhat malleable. This could produce binding that is both non-specific and relatively weak. At high concentrations of exogenous ligand, the added ligand would compete with protein side chains for binding to the heme iron. Thus, protein flexibility might enable additional molecules of ligand to penetrate the heme site of the protein, and modulate the redox

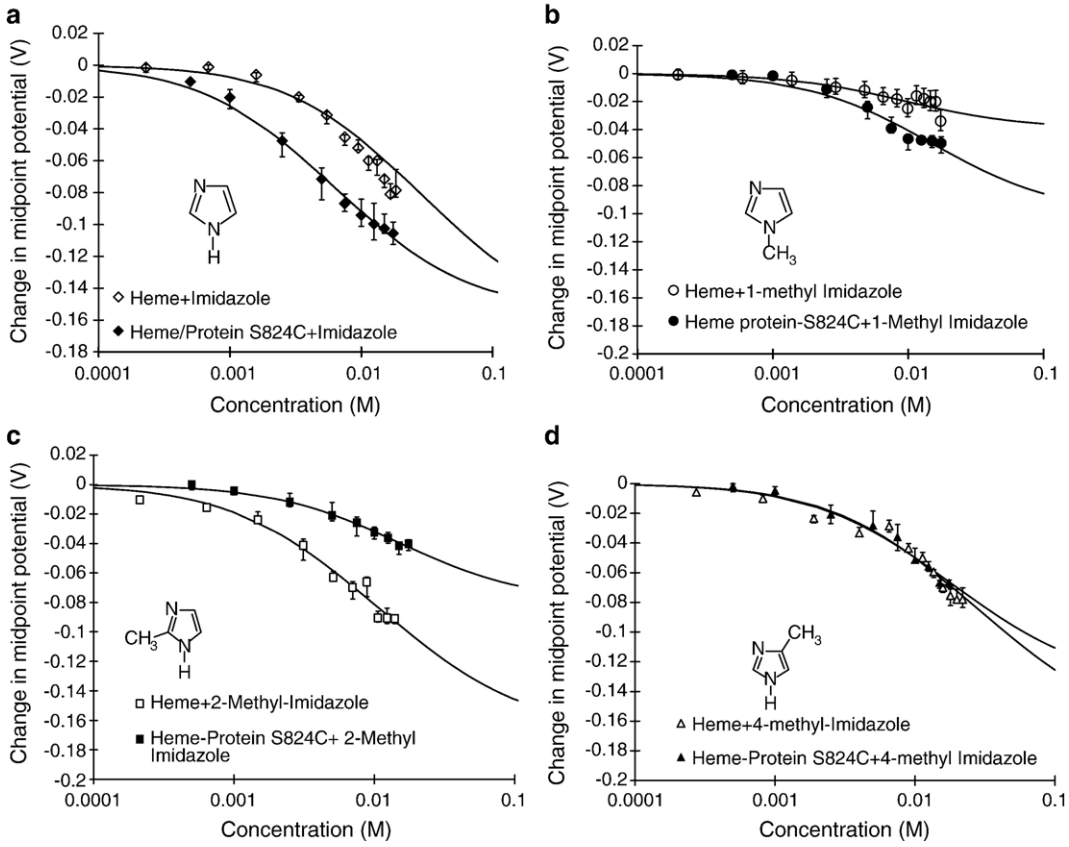

Fig. 8. Voltammetric titration of immobilized heme/S824C and isolated heme with imidazole derivatives. The observed net reduction potentials were plotted against the logarithm of the concentration of ligand. The binding profiles are plotted for (a) imidazole (diamonds), (b) 1-methyl imidazole (circles), (c) 2-methyl-imidazole (squares) and (d) 4-methyl imidazole (triangles). The curves are the computed nonlinear regression fit to the equation $\Delta E_m=(mRT/F)\ln[(1+K_{red}[S])/(1+K_{ox}[S])]$ where $\Delta E_m=E_{bound}-E_{free}$ and m is the number of ligand molecules bound to the heme center. The ratio of the K_{ox}/K_{red} obtained from the fit is listed in Table 1.

potential of the heme–protein in a non-specific (broad) and more heterogeneous manner than is seen for natural heme proteins [21,22].

2.3.4. Differential binding of oxidized and reduced heme to N-donor molecules

Our finding that each ligand has a somewhat different effect on the reduction potential indicates that each of these small molecules has a different effect on the equilibrium between the oxidized and reduced states of heme. This in turn indicates that each compound binds the oxidized and reduced states of the heme protein with different relative affinities [23,24]. The reduction potential of the heme–protein shifts to more negative values on addition of imidazole, and to more positive potential on addition pyridine. A negative shift in potential indicates that the oxidized state is more stabilized than the reduced state, while a positive shift indicates that binding stabilizes the reduced state. Therefore, pyridine and its analogues stabilize the ferrous (Fe^{II}) relative to the ferric (Fe^{III}) state, whereas imidazole and its analogues preferentially stabilize the ferric (Fe^{III}) state.

The shift in reduction potential is given by the following equation:

$$\Delta E_m = (mRT/F)\ln[(1 + K_{red}[S])/(1 + K_{ox}[S])]$$

where $\Delta E_m=E_{bound}-E_{free}$. K_{red} and K_{ox} are the binding constants of the reduced and oxidized forms of heme–protein for the small molecules, m is the number of ligand molecules

Table 1
Midpoint potentials and binding constant ratios

Axial ligand	ΔE_m, heme/S824C	ΔE_m, isolated heme	K_{ox}/K_{red}, heme/S824C	K_{ox}/K_{red}, isolated heme
Imidazole	−0.096 V	−0.053 V	23.437	20.00
1-Methyl imidazole	−0.045 V	−0.020 V	6.840	2.129
2-Methyl imidazole	−0.032 V	−0.090 V	4.600	24.651
4-Methyl imidazole	−0.051 V	−0.050 V	13.330	25.560
Pyridine	0.071 V	0.149 V	0.005	0.001
2-Aminopyridine	0.006 V	0.057 V	0.913	0.275
3-Aminopyridine	0.027 V	0.038 V	0.463	0.315
4-Cyanopyridine	0.065 V	0.093 V	0.220	0.080

The shifts in midpoint potential (ΔE_m) upon addition of 0.01 M N-donor compounds are shown as ΔE_m where $\Delta E_m=E_{bound}-E_{free}$ and E_{bound} and E_{free} represent the reduction potentials in presence and absence of N-donor molecule at 0.01 M concentration. Samples were at pH 7.4 and 50 mM PBS buffer. The ratio of binding constants (K_{ox}/K_{red}) is shown, where K_{ox} and K_{red} represent binding constants of oxidized and reduced forms of the heme in either heme/S824C (column 4) or isolated heme (column 5). These values were obtained from the nonlinear regression fit of the data in Figs. 8 and 10 to the equation shown in the text.

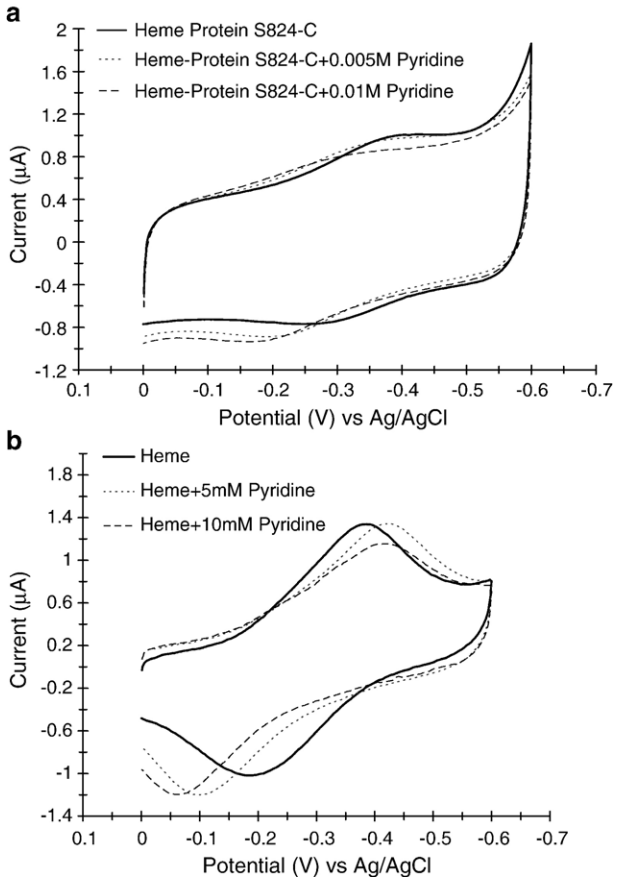

Fig. 9. (a) Cyclic voltammetry of immobilized heme/S824C in the absence (solid) and presence of 0.005 M (dotted) and 0.01 M pyridine (dashed) (scan rate 0.02 V/s). (b) Cyclic voltammetry of immobilized heme in the absence (solid) and presence of 0.005 M (dotted) and 0.01 M pyridine (dashed) (scan rate 0.02 V/s).

bound, and [*S*] is the substrate concentration. From Figs. 8 and 10, the nonlinear regression fit to this equation enables calculation of the ratios of K_{ox}/K_{red} listed in Table 1.

3. Discussion

Protein S824C was derived from a library of sequences that was not explicitly designed to bind heme. Thus, the electrochemical properties of heme/S824C can be considered as 'default' values for heme–proteins that were neither selected by evolution nor designed computationally. These default properties can later be optimized for specified technological uses though rational design and/or high throughput screening.

The high-resolution structure of S824 was solved in the apo-state [6]. As per the binary code design strategy, the histidine residues in this structure are exposed to solvent (Fig. 1). In the presence of heme, however, these residues presumably adjust their locations to accommodate the heme. While the heme site in S824C is likely to be less buried than in natural heme proteins like myoglobin, the relative insensitivity of the reduction potential of heme/S824C to ionic strength suggests that the iron is partially buried.

Binding of small N-donor molecules to this partially buried heme shifts the potential of heme/S824C (Figs. 7–10). The observed shifts upon binding to heme/S824C were distinctly different from the shifts observed upon binding of the same compounds to isolated heme.

A shift in potential indicates that binding of the N-donor ligand favors one redox state relative to the other. Several factors are known to affect which state is stabilized by such binding [23]. Shifts in potential are related both to the σ-donor/π-acceptor properties of the ligand (affecting the enthalpic term) and to the effect of water exclusion, which exerts a dual enthalpic/entropic role. Additionally, the binding of N-donor ligands by ferric and ferrous porphyrins depends on ligand basicity. In the ferric porphyrin, the stability of the N-donor heme complex increases with the basicity of the ligand and its ability to donate electron density to the metal. In contrast, for the more electron rich ferrous porphyrin, greater stability occurs for ligands that have an electron withdrawing group and can accept electron density from the metal. Thus, the reduction potential becomes more negative with an increase in ligand basicity.

Pyridine and its derivatives are readily coordinated by ferrous porphyrins as can be seen from the increase in the reduction potential upon binding (Fig. 8). Both σ bonding from the pyridine nitrogen to the iron and π-back-donation from the iron to the ligand contribute to the strength of bonding. For imidazole, σ-donor properties are much more significant than π-acceptor properties when coordinating to ferrous porphyrins, but imidazoles become better π-donors to ferric porphyrins since they can donate to the hole in the d_{xz}, d_{yz} orbitals of the iron in the ferric state. Hence, there is a direct correlation between ligand basicity and the shift in heme potential on coordination of N-donor molecules.

Our observation that heme/S-824C and isolated heme respond differently shows that the protein scaffold modulates the binding of N-donor ligands to the partially buried heme. Our results can be compared to earlier studies using microperoxidase, a 12-residue heme peptide (with no buried heme pocket), which demonstrated that the redox potential of an immobilized heme/peptide complex could be shifted by the presence of imidazoles [21,22,25]. We see that the shift in the potential on addition of N-donor ligands to heme/S-824C is less than it is for microperoxidase but more than it is for myoglobin. This suggests that protein S-824C is an intermediate case where the heme binding site is more exposed than it is in myoglobin, but less exposed than in microperoxidase.

The affinity of an iron porphyrin for N-donor ligands can be modulated by steric effects and/or by hydrogen bonding with residues near the binding site. Myoglobin, which has a buried and well-ordered heme site, binds imidazole with a lower affinity than does microperoxidase, with its solvent exposed heme and open coordination site [26]. Exposure of the heme in S824C is likely to be greater than in myoglobin, but less than in microperoxidase or isolated heme. Heme/S824C binds imidazole and 1-methyl imidazole with greater affinity than does isolated heme. This finding suggests that hydrogen bonding interactions between imidazole (or 1-methyl imidazole) and the protein scaffold of S824C may compensate for steric costs associated with inserting the compound into the partially buried site.

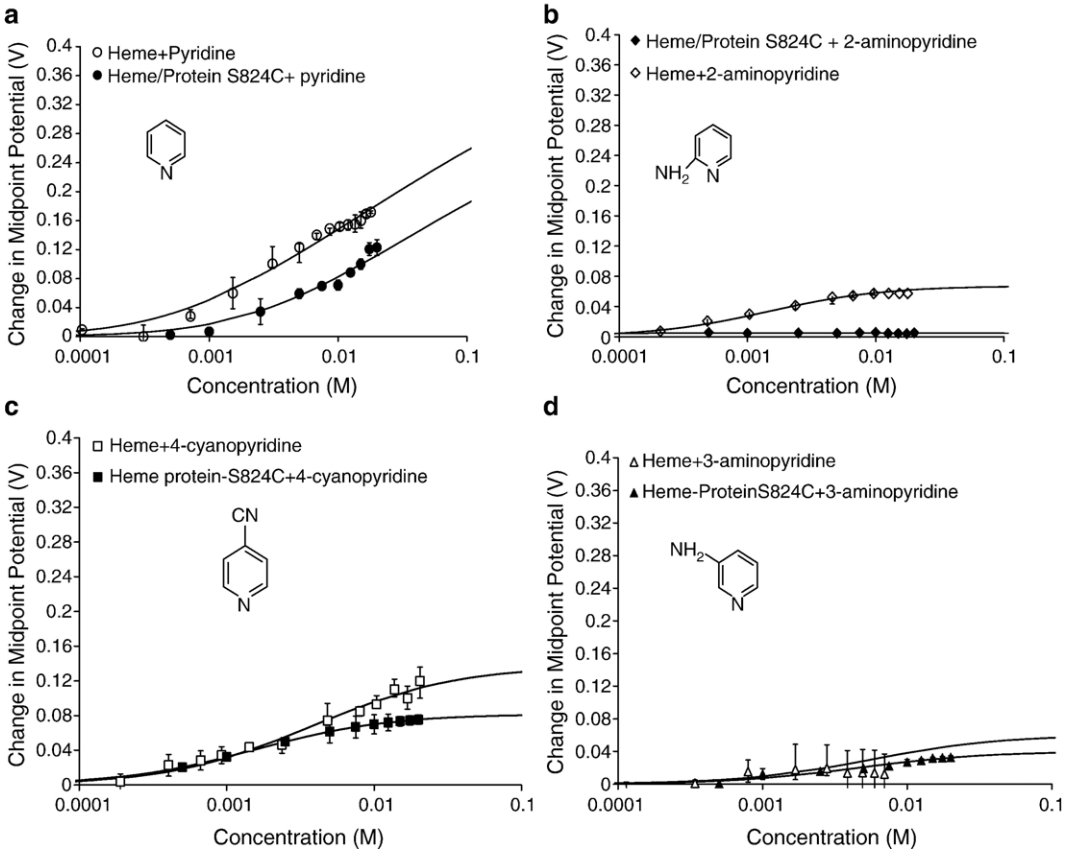

Fig. 10. Voltammetric titration of immobilized S-824-C/heme and isolated heme with pyridine derivatives. The observed net reduction potentials were plotted against the logarithm of the concentration of ligand. The binding profiles are plotted for (a) pyridine (circles), (b) 2-aminopyridine (diamonds), (c) 4-cyanopyridine (squares) and (d) 3-aminopyridine (triangles). The curves are the computed nonlinear regression fit to the equation $\Delta E_m=(mRT/F)\ln[(1+K_{red}[S])/(1+K_{ox}[S])]$ where $\Delta E_m=E_{bound}-E_{free}$ and m is the number of ligand molecules bound to the heme center. The ratio of the K_{ox}/K_{red} obtained from the fit is listed in Table 1.

For 2-methyl imidazole the situation is different. This compound binds isolated heme better than S-824C/heme. Apparently the methyl group on the 2 position sterically (or otherwise) clashes with the protein scaffold.

For pyridine and its derivatives, binding to heme/S824C is weaker than binding to isolated heme. Indeed, for 2-aminopyridine the protein blocks binding entirely. Interference by the protein scaffold with pyridine binding is similar to what has been observed for myoglobin, which does not bind pyridine [26]. Apparently, because pyridine cannot hydrogen bond to the protein, it cannot overcome the steric cost associated with insertion into a (partially) buried binding site.

3.1. Conclusions and future prospects

The experiments described above demonstrate that a de novo protein from a designed binary patterned library (i) can be immobilized on a gold electrode; (ii) binds heme; and (iii) generates an electrochemical signal. Moreover, (iv) binding of small molecules (pyridines and imidazoles) shifts the reduction potential of heme–protein; (v) this shift in potential is sensitive to changes in the concentration of the small molecules; and (vi) responds differently to different pyridine and imidazole derivatives. Additionally, (vii) the effect of binding of N-donor molecules to heme/S824C is different from binding of the same compounds to isolated heme, thereby demonstrating that the scaffold of the de novo protein modulates the affinity of small molecules for the heme moiety.

Natural heme proteins like myoglobin typically have heme pockets that are buried and not readily accessible to N-donor molecules. At the other extreme, heme bound peptides, such as microperoxidase, have exposed hemes with unhindered binding pockets, wherein the scaffold plays little role in binding. In contrast, as shown above, de novo heme proteins from combinatorial libraries can have intermediate properties wherein the heme is not only accessible enough to allow binding, but also embedded enough in the protein to enable the surrounding residues to modulate binding and discriminate between different small molecule analytes. These features can be exploited in future work toward the design of biosensors that can detect and discriminate between biologically relevant N-donor molecules such as serotonin and histamine.

4. Materials and methods

4.1. Materials

Pyridine and imidazole were purchased from Merck. 4-Cyanopyridine, 2-amino-pyridine, 3-aminopyridine, 1-methyl imidazole, 2-methyl imidazole, 4-methyl-imidazole, cystamine

(2,2′-diaminodiethyldisulphide), 1,12-diaminododecane, 3,3′-dithiopropionic acid di-(*N*-succinimidyl ester), 3-carboxypropyl disulphide and 1-ethyl-3-(3-dimethylaminopropyl)carbodiimide (EDC) were from Adrich-Sigma-Fluka. Heme (choloroprotoporphyrin IX iron (III)) (H-5533) was from Aldrich-Sigma-Fluka. The buffer salts ($KH_2PO_4{\cdot}3H_2O$ and KH_2PO_4) were of analytical grade and DMSO was obtained from Fisher Scientific. *N*-Succinimidyl-3-maleimidopropionate was from Pierce. The reference and auxiliary electrodes were from Bioanalytical systems Inc. (West Lafayette, IN).

4.2. Mutagenesis of sequence S824 and protein expression

DNA encoding protein S824 was modified using PCR to encode an additional glycine–glycine–cysteine tripeptide at the C terminus of the protein sequence. The resulting protein, S824C was expressed using the pET system in *E. coli* strain BL21(DE3) [27], and purified using published methods [5,6,28]. Dithiothreitol (DTT, 1 mM) was added to prevent formation of disulphide bonds. Purified proteins were concentrated and buffer was exchanged into 50 mM sodium phosphate buffer (pH 7.4) using Centricon Plus-20 filters (Biomax 5-Millipore). Before immobilization on the maleimide modified gold electrode, the protein was passed through a Pharmacia PD-10 column to remove DTT. The oligomerization state of the protein was assayed using size exclusion chromatography. The protein was found to be mostly monomeric in the presence of 1 mM DTT. Expression and purification of protein were evaluated by SDS-PAGE. Protein concentration was measured by UV–VIS spectroscopy using a Hewlett Packard 8452A diode array spectrophotometer.

4.3. Chemical modification of gold electrodes

Gold electrodes (0.5 mm diameter gold wire, geometrical area 1.05 cm^2) were cleaned as described by Katz and Solov'ev [29]. CV recorded in 0.5 M sulfuric acid was used to determine the purity of the electrode surface just before modification. The cleaned gold electrode was modified by soaking in 100 mM cystamine (2,2′-diaminodiethyldisulphide) in water for 2 h. The electrode was then rinsed thoroughly with water to remove physically adsorbed cystamine [30]. The electrode was further modified by immersion for 2 h into a 1-mM solution of *N*-succinimidyl-3-maleimidopropionate in DMSO [14] (Fig. 1).

4.4. Immobilization of protein onto the maleimide modified gold electrode

The heme protein was immobilized in either of two ways:

(1) Incorporation of heme into a pre-immobilized protein: The maleimide modified gold electrode was treated for 2 h with protein S824C (300 μM, in 50 mM sodium phosphate buffer, pH 7.4). This was followed by rinsing with water. The CV of the protein-modified electrode (prior to addition of heme) was recorded as a control. It showed no faradic response. Finally, the apo-protein layer was converted to heme/S824C by soaking for 2 h in 1 mM iron (III) choloroprotoporphyrin IX dissolved in 50 mM sodium phosphate buffer (pH 7.4). [Stock solutions of iron (III) choloroprotoporphyrin IX were made in 0.1 M NaOH.]

(2) Immobilization of a pre-formed heme protein: Incorporation of Fe (III)-protoporphyrin IX into protein S824C was accomplished in solution using a freshly prepared stock solution of 1–2 M heme chloride (Sigma). Aliquots of this stock solution were added to the protein samples until the ratio of the Soret band at 413 nm to the free heme band at 356 nm reached maximum Moffet et al. [13]. The maleimide functionalized gold electrode (see above) was then treated with this reconstituted protein for 4 h. The advantage of this second method is that the potential observed in the CV experiments must result from heme bound to protein S824C, and not from heme bound on cystamine or some other heme/electrode complex. Both the methods of immobilization give similar results in the cyclic voltammetry experiments.

4.5. Immobilization of heme on gold electrode

Heme was attached to the electrode using published methods with minor modifications [20]. The cleaned electrodes were immersed into a 100-mM solution of thiols in DMSO. After incubation for 90 min at room temperature, the electrodes were thoroughly rinsed with water and then immersed into 20 mM 1,12-diaminododecane. The C_{12} spacer (1,12 diaminodecane) was used for all the proteins. After 4 h, the electrodes were thoroughly washed with water and transferred to heme coupling solution. Heme was dissolved in DMSO for a final concentration of 1 mM and then diluted 10 times in 10 mM pH 7.8 HEPES buffer containing 150 mM EDC (1-ethyl-3-(3-dimethylaminopropyl) carbodiimide) coupling agent. The heme coupling was done overnight at 4 °C. The electrodes were rinsed with distilled water.

4.6. Cyclic voltammetry

Cyclic voltammograms were recorded in 50 mM sodium phosphate buffer at pH 7.4 using either a BAS 100B/W Electrochemical Workstation or CH instruments model 660 electrochemical workstation. All measurements were performed at ambient temperature (~22 °C) in a conventional three-compartment electrochemical cell consisting of the chemically modified gold electrode as a working electrode, a platinum auxiliary electrode and a saturated Ag/AgCl/KCl electrode as the reference. Oxygen was removed from the solution in the electrochemical cell by purging with Argon for several minutes before recording the CV. All potentials are reported with respect to the Ag/AgCl/KCl reference electrode.

4.7. Binding of ligands

Solutions of N-donor molecules were in milli-molar concentrations (Table 1). The pH was maintained at 7.4 with

50 mM phosphate buffer. Titrations of ligand were performed by adding aliquots of each to 10 mL of buffer in the electrode sample cell. Correction was not made for the effect of added ligands on the pH value of the buffer solution. The sample cell was purged thoroughly with Argon and each addition was allowed to equilibrate for few minutes before recording the cyclic voltammogram.

References

[1] L. Gorton, A. Lindgren, T. Larsson, F.D. Munteanu, T. Ruzgas, I. Gazaryan, Direct electron transfer between heme-containing enzymes and electrodes as basis of third generation biosensors, Anal. Chim. Acta 400 (1999) 91–108.

[2] P. McFadden, Broadband Biodetection: Holmes on a chip, Science 297 (2002) 2075–2077.

[3] H.W. Hellinga, J.S. Marvin, Protein engineering and the development of generic biosensors, Trends Biotechnol. 16 (1998) 183–189.

[4] G. Gilardi, A. Fantuzzi, Manipulating redox systems: application to nanotechnology, Trends Biotechnol. 19 (2001) 468–476.

[5] Y. Wei, T. Liu, S.L. Sazinsky, D.A. Moffet, I. Pelczer, M.H. Hecht, Stably folded de novo proteins from a designed combinatorial library, Protein Sci. 12 (2003) 92–102.

[6] Y. Wei, S. Kim, D. Fela, J. Baum, M.H. Hecht, Solution structure of a de novo protein from a designed combinatorial library, Proc. Natl. Acad. Sci. U. S. A. 100 (2003) 13270–13273.

[7] S. Kamtekar, J.M. Schiffer, H. Xiong, J.M. Babik, M.H. Hecht, Protein design by binary patterning of polar and nonpolar amino acids, Science 262 (1993) 1680–1685.

[8] M.W. West, W. Wang, J. Patterson, J.D. Mancias, J.R. Beasley, M.H. Hecht, De novo amyloid proteins from designed combinatorial libraries, Proc. Natl. Acad. Sci. U. S. A. 96 (1999) 11211–11216.

[9] M.H. Hecht, A. Das, A. Go, L. Bradley, Y. Wei, De novo proteins from designed combinatorial libraries, Protein Sci. 13 (2004) 1711–1723.

[10] N.R.L. Rojas, S. Kamtekar, C.T. Simons, J.E. McLean, K.M. Vogel, T.G. Spiro, R.S. Farid, M.H. Hecht, De novo heme proteins from designed combinatorial libraries, Protein Sci. 6 (1997) 2512–2524.

[11] D.A. Moffet, L.K. Certain, A.J. Smith, A.J. Kessel, K.A. Beckwith, M.H. Hecht, Peroxidase activity in heme proteins derived from a designed combinatorial library, J. Am. Chem. Soc. 122 (2000) 7612–7613.

[12] D.A. Moffet, M.A. Case, J.C. House, K. Vogel, R.D. Williams, T.G. Spiro, G.L. McLendon, M.H. Hecht, Carbon monoxide binding by de novo heme proteins derived from designed combinatorial libraries, J. Am. Chem. Soc. 123 (2001) 2109–2115.

[13] D.A. Moffet, J. Foley, M.H. Hecht, Midpoint reduction potentials and heme binding stoichiometries of de novo proteins from designed combinatorial libraries, Biophys. Chemist. 105 (2003) 231–239.

[14] I. Willner, V. Heleg-Shabtai, E. Katz, H.K. Rau, W. Haehnel, Integration of a reconstituted de novo synthesized hemoprotein and native metalloproteins with electrode supports for bioelectronic and bioelectrocatalytic applications, J. Am. Chem. Soc. 121 (1999) 6455–6468.

[15] E. Laviron, General expression of the linear potential sweep voltammogram in the case of diffusionless electrochemical systems, J. Electroanal. Chem. 101 (1979) 19–28.

[16] E. Laviron, L.J. Roullier, General expression of the linear potential sweep voltammogram for a surface redox reaction with interactions between the adsorbed molecules: applications to modified electrodes, J. Electroanal. Chem. 115 (1980) 65–74.

[17] D.L. Pilloud, X. Chen, P.L. Dutton, C.C. Moser, Electrochemistry of self-assembled monolayers of iron protoporphyrin IX attached to modified gold electrodes through thioether linkage, J. Phys. Chem., B 104 (2000) 2868–2877.

[18] D.K. Das, J. Medhi, The role of heme propionate in controlling the redox potential of heme: square wave voltammetry of protoporphyrinato IX iron (III) in aqueous surfactant micelles, J. Inorg. Biochem. 70 (1998) 83–90.

[19] P.D. Barker, J.L. Butler, P.D. Oliveira, H.A.O. Hill, N.I. Hunt, Direct electrochemical studies of cytochrome b_{562}, Inorg. Chim. Acta 252 (1996) 71–77.

[20] H. Zimmermann, A. Lindgren, W. Schuhmann, L. Gorton, Anisotropic orientation of horseradish peroxidase by reconstitution on a thiol-modified gold electrode, Chemistry 6 (2000) 592–599.

[21] H.M. Goldston, A.N. Scribner, S.A. Trammell, L.M. Tender, A model recognition switch. Electrochemical control and transduction of imidazole binding by electrode-immobilized microperoxidase-11, Chem. Commun. 7 (2002) 416–417.

[22] W. Zhang, F. Chunhai, S. Yuting, G. Li, An electrochemical investigation of ligand-binding abilities of biomimetic membrane-entrapped myoglobin, Biochim. Biophys. Acta Gen. Subj. 1623 (2003) 29–32.

[23] G. Battistuzzi, M. Borsari, J.A. Cowan, A. Ranieri, M. Sola, Control of cytochrome *c* redox potential: axial ligation and protein environment effects, J. Am. Chem. Soc. 124 (2002) 5315–5324.

[24] J.M. Shifman, B.R. Gibney, R.E. Sharp, P.L. Dutton, Heme redox potential control in de novo designed four alpha helix bundle proteins, Biochemistry 39 (2000) 14813–14821.

[25] H.M. Marques, I. Cukrowski, P.R. Vashi, Coordination of weak field ligands by *N*-acetylmicroperoxidase-8 (NAcMP8), a ferric haempeptide from cytochrome *c*, and the influence of the axial ligand on the reduction potential of complexes of NacMP8, J. Chem. Soc., Dalton Trans. 8 (2000) 1335–1342.

[26] C.B. Perry, T. Chick, A. Ntlokwana, G. Davies, H.M. Marques, The co-ordination of ligands by iron porphyrins: a comparison of ligand binding by myoglobin from sperm whale and the haem undecapeptide from cytochrome *c*, J. Chem. Soc. Dalton Trans. 3 (2002) 449–457.

[27] F.W. Studier, A.H. Rosenberg, J.J. Dunn, J.W. Dubendorff, Use of T7 RNA polymerase to direct expression of cloned genes, Methods Enzymol. 185 (1990) 60–89.

[28] B.H. Johnson, M.H. Hecht, Recombinant proteins can be released from *E. coli* cells by repeated cycles of freezing and thawing, Biotechnology 12 (1994) 1357–1360.

[29] E.Y. Katz, A.A. Solov'ev, Chemical modification of platinum and gold electrodes by naphthoquinones using amines containing sulphhydryl or disulphide groups, J. Electroanal. Chem. 291 (1990) 171–186.

[30] E.Y. Katz, D.D. Schlereth, H.L. Schmidt, Electrochemical study of pyrroloquinoline quinone covalently immobilized as a monolayer onto a cystamine-modified gold electrode, J. Electroanal. Chem. 367 (1994) 59–70.